



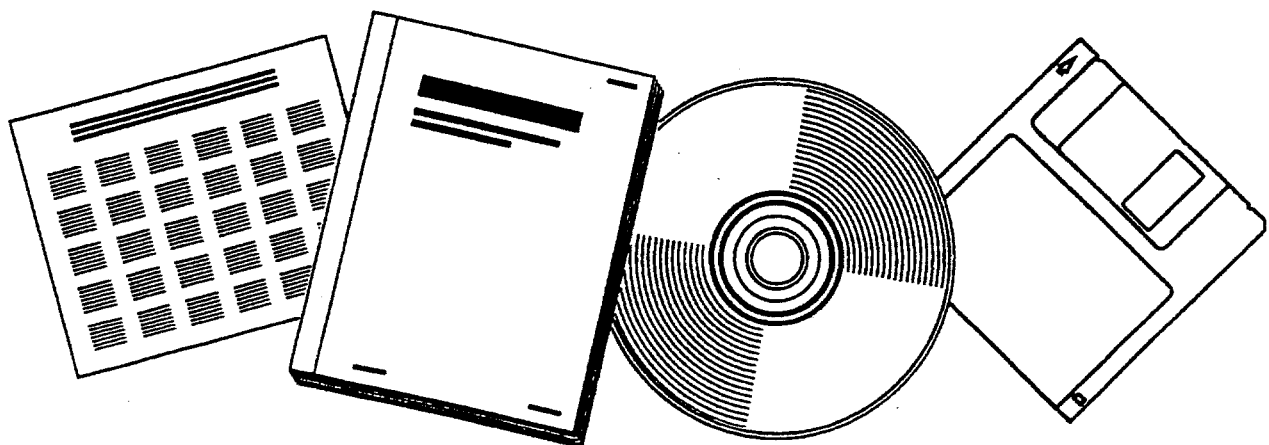
DE85010605

NTIS
Information is our business.

DEVELOPMENTS IN INDIRECT COAL LIQUEFACTION IN SLURRY-PHASE AND OTHER REACTION SYSTEMS

CATALYTICA ASSOCIATES, INC.
MOUNTAIN VIEW, CA

FEB 1984



U.S. DEPARTMENT OF COMMERCE
National Technical Information Service

COPY

Developments in Indirect Coal Liquefaction in
Slurry-phase and Other Reaction Systems

Prepared by

Catalytica Associates, Inc.
430 Ferguson Drive, Bldg. 3
Mountain View, California 94043

Principal Investigators
Ken K. Ushiba
Jacques C. De Deken

Submitted to

United States Department of Energy
Contract No. DE-AC01-81FE-05077

February 1984
Catalytica File No. 3164-3

ABSTRACT

This report accounts for Task 3 of DOE Contract No. DE-AC01-81FE-05077. It reviews the developments in indirect coal liquefaction with emphasis on slurry-phase reactors and catalysis. This report also discusses of topics related to indirect coal liquefaction research, such as analytical techniques in catalysis. The subjects covered in this report were selected by DOE.

This report is the third and final task report of the three major tasks in this contract. The first task, "Direct Coal Liquefaction Catalyst Development--Program Review and Research Perspectives," was completed in November 1982. The second task, "Review of Direct Coal Liquefaction by Slurry-Phase Catalysis," was completed in September 1983.

Table of Contents

	<u>Page</u>
Abstract	iii
1. Summary and Recommendations	1-1
1.1 Slurry Reactor	1-1
1.2 Catalytic Functions	1-1
1.3 Economics of Advanced Technologies	1-3
1.4 Solvent Effects in Slurry Reactions	1-5
1.5 Analytical Contributions	1-7
1.6 Strong Metal-support Interactions	1-8
1.7 CO ₂ as a By-product of Slurry Reaction	1-12
1.8 The Schulz-Flory Mechanism	1-12
2. Introduction	2-1
3. Improvements in the Use of Carbon Monoxide/Hydrogen Mixtures	3-1
3.1 General Perspective	3-1
3.2 Developments in Fuel Synthesis via Methanol	3-3
3.2.1 Introduction	3-3
3.2.2 Developments in Catalysts for Methanol Synthesis	3-6
3.2.3 Conclusions	3-14
3.3 Developments in Fuel Synthesis via Fischer-Tropsch Catalysis . . .	3-15
3.3.1 Introduction	3-15
3.3.2 Improvements in Fischer-Tropsch Catalysis	3-16
3.3.3 Conclusions	3-19
3.4 Oxo Process Implications for Fischer-Tropsch Technology	3-21
3.4.1 Background	3-21
3.4.2 Implications for Fischer-Tropsch Development	3-24
4. Assessment of Slurry-phase Reaction Systems in Fischer-Tropsch Synthesis	4-1
4.1 Introduction	4-1
4.2 Reactor Developments	4-2
4.3 Hydrogen-to-Carbon Monoxide Ratio in Slurry-phase Operation	4-9
4.4 Identification of Scale-up and Design Problems	4-16
4.4.1 Flow Regimes	4-16
4.4.2 Degree of Phase Mixing	4-22
4.4.3 Other Important Design Parameters and Physicochemical Properties	4-23

Table of Contents
(continued)

	<u>Page</u>
4.5 Conclusions	4-26
4.6 List of Symbols	4-29
5. Economics of Indirect Liquefaction	5-1
5.1 SASOL Economics	5-1
5.2 Advanced Gasifiers	5-7
5.3 CO Shift	5-16
5.4 Advanced Synthesis Processes	5-19
5.5 Summary and Conclusions	5-27
6. Strong Metal-support Interactions (SMSI)	6-1
6.1 General Characterization	6-1
6.2 Hydrogen Chemisorption under SMSI	6-4
6.3 CO Chemisorption under SMSI	6-12
6.4 Reversibility of SMSI	6-15
6.5 Platinum on Titanium Oxide	6-21
6.6 Rhodium on Titanium Oxide	6-29
6.7 SMSI in CO/H ₂ Reactions	6-29
7. Analytical Methods	7-1
7.1 Electron Spectroscopy for Chemical Analysis (ESCA)	7-1
7.2 Auger Electron Spectroscopy (AES)	7-4
7.3 Secondary Ion-mass Spectroscopy (SIMS)	7-14
7.4 Scanning Electron Microscopy and Energy Dispersive Spectroscopy (SEM/EDS)	7-17
7.5 Summary and Conclusions	7-29
8. Schulz-Flory Limitations	8-1
8.1 Schulz-Flory Distribution	8-1
8.2 Non-Schulz-Flory Distribution	8-11
8.2.1 Synfuel Options	8-11
8.2.2 Chain Reactivity	8-16
8.2.3 Catalyst or Reactor Nonuniformity	8-16
8.2.4 Product Incorporation in Chain	8-17
8.2.5 Production of Oxygen-containing Products	8-17
8.3 Experimental Artifacts	8-18
8.3.1 Product Condensation in Reactor	8-20
8.3.2 Product Fractionation in Reactor and Receivers	8-23
8.3.3 Recommended Solutions	8-23

Table of Contents
(continued)

	<u>Page</u>
8.4 Experimental Observations	8-25
8.4.1 Union Carbide	8-25
8.4.2 Air Products and Chemicals	8-35
8.4.3 Olefin Incorporation	8-46
8.5 Summary and Conclusions	8-53
9. References	9-1

List of Figures

	<u>Page</u>
1-1 Hydrogen Chemisorption on Ir on Various Supports	1-11
3-1 Schematic Representation of the Major Uses of CO/H ₂ Mixtures	3-2
3-2 Liquid-fluidized (Ebullating) and Liquid-entrained (Slurry) Operation Modes for Air Products/Chem Systems' Liquid-phase Methanol Process Development Unit	3-5
3-3 Dependency of the Hydrocarbon Weight Fraction on the Hydrocarbon Number for a Supported Molecular Cluster Catalyst B and a Sintered Baseline Fe ₂ O ₃ Catalyst Promoted with 2% Al ₂ O ₃ , 0.5% K ₂ O, and 0.7% CaO	3-18
3-4 Yields of C ₂ -C ₄ Hydrocarbons on Fe/Mn Catalyst (Fe/Mn = 1/6) as a Function of the Space Velocity at Various CO/H ₂ Feed Ratios and Temperatures	3-20
3-5 Heterogenization of Homogeneous Catalysts	3-25
4-1 Relationship between the Exit H ₂ /CO Ratio and the Syngas Conversion for Assumed Values of the Usage Ratio and Feed H ₂ /CO Ratio of 1.5	4-12
4-2 Dependence of the Gas and Liquid Concentrations of H ₂ and CO on the Axial Reactor Distance	4-15
4-3 Assumed Dependency of Flow Regimes on Superficial Gas Velocity and Reactor Diameter	4-18
4-4 Operational Range Diagram for a Bubble-column Reactor with Suspended Solid Matter	4-20
4-5 Effect of Liquid-phase Mixing and Catalyst Activity on Hydrogen Conversion	4-24
4-6 Gas Holdup as a Function of the Superficial Gas Velocity	4-25
4-7 Solubility of Various Gases in Paraffin Gatsch (Mixture) at 10 atm .	4-27
5-1 Grass-roots F-T Plant Base Case: Lurgi (Dry Ash)-Synthol-Wyoming Subbituminous Coal	5-3
5-2 Plant Construction Costs for Mixed-output Case	5-6
6-1 H ₂ Chemisorption versus Temperature of Activation for Supported Iridium Catalysts	6-8
6-2 Hydrogen Chemisorption Isotherms (295K) of a 2.7 wt% Ni-Grafoil Catalyst Following the Pretreatments Described in Table 6-4	6-13
6-3 H ₂ Yield From Pulses of Water Injected on Anatase-Supported Metals Reduced at 773K and 473K	6-20
6-4 Variation of Particle Size Distribution with Reduction Temperature for Pt on Titanium Oxide	6-23
6-5 Variation of Particle Size Distribution with Reduction Temperature for Pt on Aluminum Oxide	6-24

List of Figures
(continued)

	<u>Page</u>
6-6 Variation of Particle Size Distribution with Reduction Temperature for Pt on Silicon Oxide	6-25
6-7 Variation of Particle Size Distribution with Reduction Temperature for Pt on Carbon	6-26
6-8 Particle Size Distribution of Pt Crystallites after Consecutive Treatments in Various Environments	6-28
6-9 Ethane Hydrogenolysis as a Function of Dispersion	6-30
6-10 n-Butane Hydrogenolysis as a Function of Dispersion	6-31
6-11 Cyclohexane Hydrogenolysis/Dehydrogenation as a Function of Dispersion	6-32
6-12 Relative Rates of Ni(CO) ₄ Formation for Ni/SiO ₂ and Ni/TiO ₂ Catalysts	6-35
7-1 Schematic of the Experimental Configuration Used for the Direct Surface Examination of Reacted Catalyst Samples by XPS	7-3
7-2 Schematic of UHV Surface Analysis System Equipped with Sample Isolation Cell for High-pressure (1-20 atm) Catalytic Studies	7-7
7-3 Comparison of Product Distributions Obtained over Initially Clean Polycrystalline Iron and Rhodium Foils	7-8
7-4 Auger Spectra of the Iron Surface before and after 30 min and after 4 h of Reaction	7-9
7-5 Schematic of UHV Apparatus with Attached Sample Transfer System and Microreactor for Catalytic Rate Measurements	7-11
7-6 Carbon 1s XPS Data After Reaction	7-12
7-7 Carbon Auger Spectra of the Three Carbonaceous Surface Phases Formed after the CO/H ₂ Reaction at 1 Bar and CO/H ₂ = 1:20	7-13
7-8 Schematic Diagram of the Spectrometer Chamber Showing the SIMS, Sample Carousel, Liquid Nitrogen Cooling System, and Ion Bombardment Gun	7-15
7-9 Schematic of a SIMS with Mass-selected Primary Ion Beam	7-16
7-10 SEM Illumination System Showing the Parts of the System that Can Usually Be Controlled by the Operator	7-20
7-11 Growth-rate Curves for Filamentous Carbon from Nickel-, Iron-, and Cobalt-catalyzed Decomposition of Acetylene	7-23
7-12 Variation of Particle Displacement Rate with Particle Radius for Silver Heated in 2.0 torr Hydrogen at 365°C	7-25
7-13 Variation of Palladium Average Particle Size with Temperature in Various Gaseous Environments (Graphite Support)	7-27
8-1 Hydrocarbon Distribution from Schulz-Flory Polymerization (Degree of Polymerization from 2 to 8)	8-5
8-2 Hydrocarbon Distribution from Schulz-Flory Polymerization (Degree of Polymerization from 6 to 15)	8-6
8-3 S-F Distribution: Weight Percent of Most Abundant Components at each D Value	8-7

List of Figures
(continued)

	<u>Page</u>
8-4 Variation of Typical Product Split with Degree of Polymerization	8-8
8-5 Hydrocarbon Product Distribution for Iron Catalysts	8-9
8-6 Product Distribution of F-T Reactions Over CO Catalyst	8-12
8-7 Hydrogen Product Distribution for a Cobalt Catalyst	8-13
8-8 One-step Synfuel Production Options	8-15
8-9 S-F Alcohol Distribution Plotted as Mole Fraction	8-19
8-10 Calculated Product Distribution Exiting Reactor, Assuming Vapor-liquid Equilibrium is Obtained Twice with Intermediate Hydrocarbon Vapor Removal	8-22
8-11 Calculated Product Fractions Collected in Successive Vessels, Assuming 50% Conversion of CO + H ₂ and Vapor-liquid Equilibrium Obtained in Each Vessel	8-24
8-12 Plot of the Hydrocarbon Product Distribution for UCC Sample No. 10011-14-07	8-26
8-13 Berty Reactor	8-34
8-14 Continuous, Automated Fischer-Tropsch Slurry Reactor	8-36
8-15 Hydrocarbon Weight Distribution for Catalyst A1	8-39
8-16 Hydrocarbon Weight Distribution for Catalyst A2 (at 237°C, 2.21 mPa)	8-40
8-17 Hydrocarbon Weight Distribution for Catalyst A2 (at 241°C, 1.12 mPa)	8-41
8-18 Hydrocarbon Weight Distribution for Catalyst B (at 247°C, 2.07 mPa)	8-42
8-19 Hydrocarbon Weight Distribution for Catalyst B (at 250°C, 2.08 mPa)	8-43
8-20 Hydrocarbon Schulz-Flory Distribution for Slurry Catalyst A2	8-44
8-21 Hydrocarbon Schulz-Flory Distribution for Fe ₂ O ₃	8-45
8-22 Hydrocarbon Weight Distribution for Fe ₂ O ₃ (at 280°C, 3.31 mPa)	8-47
8-23 Hydrocarbon Weight Distribution for Fe ₂ O ₃ (at 277°C, 3.14 mPa)	8-48
8-24 Hydrocarbon Weight Distribution for Fe ₂ O ₃ (at 281°C, 3.10 mPa)	8-49
8-25 Conversion of 2.7 mol% Added Ethylene to Ethane as a Function of Time	8-50
8-26 Comparison Between the Product Distribution Obtained from Initially Clean Fe ³⁺ with and without Added Ethylene	8-51
8-27 Product Distribution for Fixed Reaction Conductors (6 atm, 3:1 H ₂ :CO, 300°C) as a Function of Added Ethylene	8-52

List of Tables

	<u>Page</u>
1-1 Required Gasoline Selling Price	1-4
1-2 Required Gasoline Selling Price, All-liquid Mode	1-6
1-3 Hydrogen Chemisorption on TiO ₂ -supported Group VIII Noble Metals	1-10
1-4 Carbon Monoxide Chemisorption on TiO ₂ -supported Group VIII Noble Metals	1-10
3-1 Oxo Yields with Ligand and Solvent	3-23
3-2 Hydroformylation of 1-Pentene Catalyzed by P-(PPh ₂) ₃ RhH(CO), Compared with Homogeneous HRh(CO)(PPh ₃) ₃	3-26
3-3 Key Features of the Oxo and Fischer-Tropsch Processes	3-27
4-1 Reactor Technologies Applied to Fischer-Tropsch Synthesis	4-3
4-2 Major Generic Advantages of Slurry-phase Operation	4-4
4-3 Comparison of Tubular Fixed-bed, Fluidized-bed with Catalyst Entrainment, and Slurry-phase Bubble-column Operation	4-6
4-4 Some Useful Relationships Between the Feed (I), Usage (U), and Exit (E) H ₂ /CO Ratio, and the Hydrogen (X _{H₂}), Carbon Monoxide (X _{CO}), and Syngas (X _{CO+H₂}) Conversion	4-11
4-5 Feed and Usage Ratio of Hydrogen to Carbon Monoxide for Several Slurry-phase Studies of the Fischer-Tropsch Reaction	4-14
4-6 Reactor Dimensions, Superficial Velocity, and Catalyst Concentration and Size	4-19
5-1 Summary of Base Case Reactor	5-4
5-2 Construction Costs for Base Case Reactor	5-5
5-3 Construction Cost Comparison--Base Case vs. BGC Case	5-8
5-4 Comparison of Products after Downstream Processing (BGC Synthol and SASOL-U.S. for Mixed and All-liquid Output)	5-9
5-5 Comparison of Product Slates from Grass-roots F-T Plants	5-11
5-6 Construction Cost Comparisons	5-12
5-7 Prices Assumed for Products other than Gasoline	5-14
5-8 Gasoline Selling Cost for Various Synfuel Plants	5-15
5-9 CO Shift for Advanced Gasifiers in F-T Plant	5-17
5-10 Material Balance around CO Shift Reactor in BGC Case	5-18
5-11 Products after Downstream Processing (Mixed-product Case)	5-21
5-12 Products after Downstream Processing (All-liquid Case)	5-22
5-13 BGC/Kolbel Impact on Construction Cost (Mixed-output Case)	5-23
5-14 BGC/Kolbel Impact on Construction Cost (All-liquid Case)	5-24
5-15 Gasoline Costs for BGC/Kolbel and Other Cases	5-26
5-16 Gasoline Costs for a Combination of Kolbel with Gasifier (All-liquid Mode)	5-27
5-17 Required Gasoline Selling Price	5-28
5-18 Relative Liquid Yields	5-29

List of Tables
(continued)

	<u>Page</u>
6-1 Hydrogen Chemisorption on TiO ₂ -Supported Group VIII Noble Metals	6-5
6-2 Support Properties of the SMSI of Oxides	6-7
6-3 Correlation of SMSI Properties with Reducibility for Saturated Transition Metal Oxides	6-10
6-4 Reduction and Reaction Conditions for Ni-Graphite (Grafoil) Catalysts	6-11
6-5 Carbon Monoxide Chemisorption on TiO ₂ -Supported Group VIII Noble Metals	6-14
6-6 Reversibility of SMSI	6-16
6-7 Chemisorption of H ₂ and CO on 2% Pt/TiO ₂	6-17
6-8 H ₂ Chemisorption of Fresh Catalyst Samples at 300K	6-19
6-9 H ₂ Chemisorption and CO/H ₂ Reaction on Ni Catalysts	6-33
7-1 AES Features	7-5
7-2 Information Carried by Radiation Emitted from Surfaces	7-18
7-3 Relationship between Mobility Temperature of 10-nm Particles Supported on Graphite and their Bulk Melting Points	7-24
8-1 Schulz-Flory Distribution of Component Carbon, n, at Each Degree of Polymerization, D	8-4
8-2 Product Distribution of F-T Reactions Over CO Catalyst	8-10
8-3 Union Carbide Catalysts for Synfuels from Syngas	8-27
8-4 Co-UCC101 Testing (220°C, Low SV)	8-28
8-5 Co-UCC101 Testing (250°C, Low SV)	8-30
8-6 Co-UCC101 Testing (250°C, High SV)	8-32
8-7 Summary of Selected Slurry-phase Fischer-Tropsch Results	8-38